

## Optical potentials for charged-hadron-nucleus scattering: Role of Coulomb excitations

F. Cannata

*Dipartimento di Fisica dell'Università and Istituto Nazionale di Fisica Nucleare,  
Sezione di Bologna, I-40126 Bologna, Italy*

J. P. Dedonder\*

*Division de Physique Théorique, Institut de Physique Nucléaire, Orsay, France  
and Laboratoire de Physique Nucléaire, Université de Paris VII, Paris, France*

W. R. Gibbs

*Theoretical Division, Los Alamos National Laboratory, Los Alamos, New Mexico 87545*

(Received 11 December 1989)

For hadron-nucleus scattering, the projectile's Coulomb interaction induces, in optical potential approximations to multiple-scattering theories, an effective shift in the local energy at which the optical potential is evaluated. In addition, it gives rise to a contribution related to the Coulomb excitation (or deexcitation) of the target accompanied by the corresponding deexcitation (or excitation) by the strong interaction. The first effect is often referred to as the Coulomb shift of the reaction energy. We investigate more specifically the second one, which is usually neglected. The relative importance of both effects is studied for  $\pi^\pm$ -nucleus scattering at intermediate energies.

### I. INTRODUCTION

We consider the problem of the interplay between the strong and Coulomb interactions for a projectile scattering from a many-body system with special reference to pion scattering from the nuclei. At intermediate energies the pion-nucleon interaction has a very strong energy dependence due to the existence of the 3-3 resonance while the comparatively light mass of the projectile, together with the few partial waves involved in the elementary amplitude, render the problem tractable with multiple-scattering techniques. Using the two-potential formula, the full many-body scattering amplitude appears as the sum of the Rutherford scattering amplitude and a Coulomb distorted strong-interaction amplitude. Of course the second amplitude is not the same as would have been obtained in the absence of the Coulomb interaction; it is built up with intermediate-state propagation in the presence of the Coulomb field. If one averages the Coulomb potential over the single-particle coordinates, part of the Coulomb alteration of the strong interaction can be expressed as a modification of the reaction energy: a negatively charged particle is accelerated when approaching the nucleus while the motion of a positively charged projectile is retarded, resulting in a loss of kinetic energy; i.e., a  $\pi^-$  has a larger effective kinetic energy at the surface of the nucleus than a  $\pi^+$ . These effects have been extensively studied in semiclassical approaches<sup>1-5</sup> with, in particular, the aim of investigating the distribution of neutrons via phenomenological analyses of the pion-scattering data. In optical potential approximations to multiple-scattering theories, it has been argued that these Coulomb effects also lead to a modification of the reaction energy.<sup>6-10</sup> The importance of the Coulomb energy shift has been clearly illustrated in

the area of pion scattering in the resonance region.<sup>7,8</sup>

Taking into account the explicit dependence of the nuclear Coulomb field on the proton coordinates one should retain the effects of excitation (or deexcitation) of the target induced by the projectile's Coulomb interaction. To our knowledge, no study of this aspect of the Coulomb problem has been made in the context of pion scattering at low and intermediate energies except for pionic atoms. There, however, in contrast to the scattering regime presently under consideration, the Coulomb interaction is the dominant process.<sup>11</sup> It should be remarked that rather detailed analyses of the projectile's Coulomb effects have been undertaken, in the context of the three-body problem, for  $\pi$ - $d$  scattering where possible charge symmetry effects are investigated (see, for instance, Ref. 12, and references quoted therein). The usual argument for neglecting virtual Coulomb excitations in medium-energy scattering relies upon the fact that they add incoherently. This is expected to lead to a suppression of the corresponding contribution to the angular distributions in contrast to that associated with the Coulomb energy shift which reflects, as already mentioned, coherent intermediate excited states Coulomb rescatterings.

It is with the perspective of studying nuclear sizes, and more precisely of comparing neutron and proton radii, that we develop the present work concerning ourselves with the estimate of the size of the Coulomb excitation effect. The aim is to be able to set stronger bounds on the values of neutron radii extracted from the data<sup>13-16</sup> together with a realistic estimate of the theoretical errors involved. One effect which must be treated for the extraction of radii is that of true absorption,<sup>17-19</sup>

The present work will start with a formal discussion of the role of the projectile's Coulomb interaction for hadron scattering by nuclei. Within the framework of

multiple-scattering theories,<sup>20</sup> we derive the optical potential in the presence of both strong and Coulomb interaction, and show that two branches of modifications (in addition to the Rutherford scattering contribution) arise as compared to the pure strong (i.e., in the absence of projectile Coulomb interaction) optical potential. The first branch of correction is related to Coulomb rescatterings in the intermediate excited target states. The second is due to initial and/or final excitation (or deexcitation) of the target by the Coulomb interaction.

Since the first type of correction has already been studied<sup>7,8</sup> one has some idea of the magnitude of the effects to be expected. Although many questions remain open regarding the reliability of these corrections, we will, in the present work, simply use the results in Refs. 7 and 8. We shift the reaction energy by the value of the Coulomb potential at the surface of the nucleus. We will mainly address ourselves to the analysis of the virtual-Coulomb-excitation contribution. This provides a correction to the most common treatment of the Coulomb potential in the optical model which is the simple addition of a spherical potential obtained from the average over the nuclear charge density.

$$V(r) = Ze^2 \int d\mathbf{r}' \rho(\mathbf{r}') / |\mathbf{r} - \mathbf{r}'| .$$

Averaging over nucleon coordinates the Coulomb interaction between the projectile and the individual nucleons changes its quantum-mechanical operator nature. While it still acts as an operator on the projectile the dependence on single-particle nucleon coordinates disappears; hence, in this approximation, the Coulomb excitation of the nucleus by the projectile is neglected. While it is true that the virtual excitation and deexcitation of a nuclear state by the Coulomb force is a small effect, the virtual Coulomb excitation followed by a strong deexcitation is more important. The corrections to the optical potential considered here which are different for the two pionic charges take the form of an additional (complex) potential to be added to strong optical potential. We do not consider the excitation by the transverse photons which would not change the order of magnitude of our estimates in any significant way. The potential expressing Coulomb excitation is very nonlocal and has a long-range behavior (in either of the variables) which decreases as  $1/r^3$ . This asymptotic dependence on  $r$  arises from the convolution of a Green's function propagator with the long-range Coulomb potential.

The paper is organized as follows. Section II contains the formal developments underlying the construction of the ground-state optical potential in the presence of the projectile's Coulomb interaction. We display there the two major modifications brought to the strong optical potential. Section III presents a discussion of the role of virtual Coulomb excitations. There we introduce analytic expressions (of the lowest-order contribution) for these excitations which lead, within the approximation to be discussed, to expressions amenable to numerical evaluation. In Sec. IV we present numerical results, at various scattering energies, which show the influence of the Coulomb excitation correction as compared to the standard addition of the Coulomb potential and to Coulomb

energy shift modification. At this stage of our work we discuss only different theoretical approximations and no direct comparison with existing data will be made. Section V summarizes the main results of this work.

## II. FORMAL OUTLINE OF THE TREATMENT

In the study of the scattering of a charged projectile by a nucleus, the Coulomb interaction is usually treated, in potential models, as an external field which depends on the projectile's coordinate. This potential is added to a "strong" potential in a Schrödinger-like equation. It has been known, however, for some time that the effects of the Coulomb interaction are far more complex than assumed in that simple model. An illustration of this fact is given by the case of a constant (in coordinate space) potential: in a multiple-scattering approach, it would simply lead to a shift in the energy argument of the strong optical potential. It should be clear, therefore, that the long-range nature of the Coulomb interaction does not *a priori* forbid a multiple-scattering approach to this two-potential problem. However, the strong short-range interaction and the Coulomb interaction, precisely because of its long range (i.e., the projectile is affected by the presence of the Coulomb field of all the protons in the nucleus), cannot be treated on the same footing.

We start from the general Lippmann-Schwinger equation for the many-body ( $A+1$ ) transition matrix in terms of potentials acting (pairwise) between the projectile and a single nucleon:

$$T = (V_N + V_C)[1 + G_0^+(E)T] . \quad (2.1)$$

The potentials  $V_N$  and  $V_C$  are the sum of the two-body strong and Coulomb potentials

$$V_N = \sum_{i=1}^A V_N^i, \quad V_C = \sum_{j=1}^Z V_C^j . \quad (2.2a)$$

The free Green's operator in Eq. (2.1) is given by

$$G_0^+(E) = (E + i\delta - H_0)^{-1} \quad (\text{with } \delta \text{ going to zero}) , \quad (2.2b)$$

$$H_0 = H_A + K_p , \quad (2.2c)$$

where  $H_A$  is the nucleus  $A$ -body Hamiltonian and  $K_p$  the kinetic energy operator for the projectile. We define, as usual, the operator  $P_0(Q_0)$  to project onto the ground (excited) state(s) of the target ( $P_0 + Q_0 = 1$ ). Then the (many-body) optical potential operator  $U(E)$  is defined such that

$$T = [V_C + U(E)][1 + P_0 G_0(E)T] , \quad (2.3)$$

$$U(E) = V_N + (V_N + V_C) Q_0 \frac{1}{E - H_0 - Q_0(V_C + V_N)Q_0} \times Q_0(V_N + V_C) . \quad (2.4)$$

This expression (2.4) for the optical potential operator should be compared with the pure strong optical potential  $U_N(E)$  as it would arise in the absence of projectile-Coulomb interactions in Eq. (2.1), i.e.,  $V_C = 0$  in Eq. (2.4)

[see Eq. (A4)]. Hence the modified ground-state optical potential,  $P_0 U(E) P_0$ , can now be expressed in terms of the pure strong potential  $U_N(E)$ . This gives (Appendix A) the result

$$\begin{aligned} P_0 U(E) P_0 &= P_0 U_N(E - Q_0 V_C Q_0) P_0 + P_0 \Delta_C(E) P_0 \quad (2.5a) \\ &= P_0 U_N(E) P_0 + P_0 \Delta_N(E) P_0 + P_0 \Delta_C(E) P_0, \quad (2.5b) \end{aligned}$$

where the ground-state projections of  $\Delta_N(E)$  and  $\Delta_C(E)$  are given in Eqs. (A10) and (A8). As anticipated in the Introduction, we have two branches of Coulomb-induced corrections. The first one, displayed in the second term of the right-hand side (rhs) in Eq. (2.5b), represents the difference between the pure strong nuclear optical potential operator evaluated at a Coulomb shifted energy  $E - Q_0 V_C Q_0$  and at  $E$ . In spite of its innocent looking form the evaluation of this correction is far from trivial since the shift appears at the operator level. At present, let us simply comment that we may reexpress the shifted strong optical potential as a formal series in the Coulomb operator  $V_C$ :

$$\begin{aligned} U_N(E - Q_0 V_C Q_0) &= U_N(E) + U_N(E) Q_0 G_0 Q_0 V_C Q_0 U_N(E) \\ &+ \dots \quad (2.6a) \end{aligned}$$

The corrections to the pure strong optical potential  $U_N(E)$  are therefore associated with coherent Coulomb rescattering ( $Q_0 V_C Q_0$ ) in the excited intermediate states. Assuming  $V_C$  to be constant, or rather assuming the commutativity of  $V_C$  with the appropriate Green's function, one would obtain the following structure<sup>10</sup>

$$\begin{aligned} U_N(E - Q_0 V_C Q_0) &\approx U_N(E) - \langle V_C \rangle \frac{d}{dE} U_N(E) \\ &\approx U_N(E - \langle V_C \rangle), \quad (2.6b) \end{aligned}$$

which corresponds to a prescription used in practice.<sup>6</sup> It is the long-range nature and the smoothness of the Coulomb potential on the strong-interaction scale which allows us to consider such approximations. However a more detailed inspection of the formal expansion (2.6a) shows that the commutation of the Green's function and the Coulomb operator required to arrive at (2.6b) is not justified *a priori*: both operators generate nonlocalities of the same nature.

The second branch of corrections,  $P_0 \Delta_C(E) P_0$ , in Eq. (2.5a) is due to the Coulomb transition operators  $P_0 V_C Q_0$  and  $Q_0 V_C P_0$  in Eq. (2.3). The corresponding contributions are characterized by an initial Coulomb excitation from the ground state followed by Coulomb and strong rescatterings and a final deexcitation to the ground state by the strong interaction (and vice versa). Thus they involve one or two Coulomb transitions to and/or from the target ground state. The formal expression (A8) displays the structure of the various contributions. Because the Coulomb interaction is rather weak we will consider, in the following developments, a perturbative expansion of  $P_0 \Delta_C(E) P_0$  retaining only the lowest-order contribution in  $V_C$  (we neglect in particular the pure Coulomb excita-

tion piece which is very small, involving two Coulomb induced transitions). Hence we have

$$\begin{aligned} P_0 \Delta_C(E) P_0 &= P_0 U_N(E) Q_0 G_0(E) Q_0 V_C P_0 \\ &+ P_0 V_C Q_0 G_0(E) Q_0 U_N(E) P_0, \quad (2.7) \end{aligned}$$

which represents processes in which the nucleus is excited by the Coulomb potential and deexcited by the strong interaction or vice versa.

This will have to be compared with the perturbative expansion associated with the intermediate Coulomb rescatterings given by Eq. (2.6a) or (A10).

$$P_0 \Delta_N(E) P_0 \approx P_0 U_N(E) G_{0(E)} Q_0 V_C Q_0 G_0(E) Q_0 U_N(E) P_0. \quad (2.8)$$

One cannot argue any further formally and, to estimate the various corrections, one has to start from an explicit evaluation of the strong optical potential  $U_N(E)$ .

The many-body optical potential will be evaluated within a first-order theory,<sup>20-25</sup> which implies a single scattering approximation for  $U_N(E)$  with an independent particle model of the nuclear target. The ground-state matrix element of the first-order optical potential then reads

$$\langle \Phi_0 | U_N(E) | \Phi_0 \rangle = \sum_{i=1}^A \langle \psi_i | t(\omega + \epsilon_i) | \psi_i \rangle, \quad (2.9)$$

where  $\Phi_0$  describes the many-body ground state of the target, while  $\psi_i$  denotes the single-particle states (with energy  $\epsilon_i$ ) occupied in the ground state.

### III. VIRTUAL COULOMB EXCITATIONS

In order to study the lowest-order (in  $V_C$ ) contribution (2.7) to the Coulomb excitation correction (A8), i.e.,

$$\begin{aligned} \langle \Phi_0 | \Delta_C(E) | \Phi_0 \rangle &= \langle \Phi_0 | \{ U_N(E) Q_0 G_0(E) Q_0 V_C \\ &+ V_C Q_0 G_0(E) Q_0 U_N(E) \} | \Phi_0 \rangle \quad (3.1) \end{aligned}$$

we turn to an explicit representation of the matrix element (3.1). In the developments below, we mainly use coordinate space representations and the numerical calculations will be performed in this space.

The two terms in (3.1) are identical under the exchange of the projectile's coordinate; hence, from this point on, we will only write one contribution, it being implicitly understood that the second piece ( $\mathbf{r}_\pi \leftrightarrow \mathbf{r}'_\pi$ ,  $\mathbf{k}_\pi \leftrightarrow \mathbf{k}'_\pi$ ) is to be included. Using the coordinate space representation,  $\mathbf{r}_\pi(\mathbf{r}'_\pi)$  denoting the initial (final) pion coordinate and  $\psi_j$  the single-particle wave functions associated with the occupied orbitals in the ground state, we have

$$\Delta_C(E, \mathbf{r}'_\pi, \mathbf{r}_\pi) = \sum_{j=1}^Z \langle \mathbf{r}'_\pi \psi_j | \Delta_j | \psi_j \mathbf{r}_\pi \rangle. \quad (3.2)$$

The sum is restricted to the proton-occupied states because of the presence of the Coulomb operator in (3.1). Inserting and summing over intermediate proton states,  $\psi_\alpha$ , not occupied in the target ground state Eq. (3.2) reads explicitly

$$\Delta_c(E, \mathbf{r}'_\pi, \mathbf{r}_\pi) = \sum_{j=1, \alpha}^Z H_{j\alpha}(\mathbf{r}'_\pi) \int d\mathbf{r}''_\pi d\mathbf{r}_N d\mathbf{r}'_N G_0^{j\alpha}(|\mathbf{r}'_\pi - \mathbf{r}''_\pi|) \psi_\alpha^*(\mathbf{r}'_N) \langle \mathbf{r}''_\pi \mathbf{r}'_N | t(E_{\alpha j}) | \mathbf{r}_\pi \mathbf{r}_N \rangle \psi_j(\mathbf{r}_N), \quad (3.3a)$$

where we have introduced the Coulomb matrix element

$$H_{j\alpha}(\mathbf{r}'_\pi) = \langle \mathbf{r}'_\pi \psi_j | V_c | \mathbf{r}'_\pi \psi_\alpha \rangle = \int d\mathbf{r} \psi_j^*(\mathbf{r}) V_c(|\mathbf{r}'_\pi - \mathbf{r}|) \psi_\alpha(\mathbf{r}). \quad (3.3b)$$

In Eq. (3.3a), although it is diagonal in the nucleon coordinate, the Green's function must carry the index ( $j\alpha$ ) because its energy argument depends on both the initial orbital ( $\psi_j$ ) and the intermediate one ( $\psi_\alpha$ )  $E_{\alpha j} = E - E_\alpha + E_j$ . In the static approximation (i.e., the nucleon mass,  $m_N$ , becomes very large) that we shall use for the evaluation of the correction, the nucleon coordinate will be unchanged by the strong-interaction  $t$  matrix and we have, denoting by  $\tilde{\Delta}$  the static result

$$\tilde{\Delta}_c(E, \mathbf{r}'_\pi, \mathbf{r}_\pi) = \sum_{j=1, \alpha}^Z H_{j\alpha}(\mathbf{r}'_\pi) \int d\mathbf{r}''_\pi d\mathbf{r}_N G_0^{j\alpha}(|\mathbf{r}'_\pi - \mathbf{r}''_\pi|) \psi_\alpha^*(\mathbf{r}_N) \langle \mathbf{r}''_\pi - \mathbf{r}_N | t(E_{\alpha j}) | \mathbf{r}_\pi - \mathbf{r}_N \rangle \psi_j(\mathbf{r}_N). \quad (3.4)$$

In many cases the restriction on the sum over the intermediate states  $\psi_\alpha$  (i.e.,  $Q_0 = 1 - P_0 \neq 1$ ), which is also referred to as the Pauli blocking correction,<sup>27,28</sup> is not crucial. Although it might seem to be unimportant for the computation of what is expected to be a small correction, it is in fact essential. Indeed, relaxing this restriction on the summation Eq. (3.4) would lead to an incorrect long-range behavior. This is qualitatively clear from the fact that  $P_0 V_c P_0$  behaves like  $1/r_\pi$  for large  $r_\pi$  while the transition contribution,  $Q_0 V_c P_0$ , falls off at least as  $1/r_\pi^2$ . In the present work the evaluation of  $\tilde{\Delta}_c(E)$  was done by summing over the complete set of intermediate states and by subtracting explicitly the contribution of the ground-state orbitals. We now proceed in two steps and consider first the closure (i.e., sum over all intermediate states) contribution. Neglecting the energy dependence related to the nuclear states in Eq. (3.4) we obtain

$$\begin{aligned} \tilde{\Delta}_c(E, \mathbf{r}'_\pi, \mathbf{r}_\pi) &= \sum_{j=1}^Z \int d\mathbf{r}''_\pi d\mathbf{r} |\psi_j(r)|^2 V_c(|\mathbf{r}'_\pi - \mathbf{r}|) \\ &\quad \times G_0(|\mathbf{r}'_\pi - \mathbf{r}''_\pi|) \\ &\quad \times \langle \mathbf{r}''_\pi - \mathbf{r} | t(E) | \mathbf{r}_\pi - \mathbf{r} \rangle \end{aligned} \quad (3.5a)$$

or, equivalently in momentum space

$$\begin{aligned} \tilde{\Delta}_c(E, \mathbf{k}'_\pi, \mathbf{k}_\pi) &= \sum_{j=1}^Z F_j(\mathbf{k}'_\pi - \mathbf{k}_\pi) \int \frac{d\mathbf{k}}{(2\pi)^3} V_c(|\mathbf{k}'_\pi - \mathbf{k}|) \\ &\quad \times G_0(k) \langle \mathbf{k} | t(E) | \mathbf{k}'_\pi \rangle, \end{aligned} \quad (3.5b)$$

where

$$F_j(\mathbf{q}) = \int \frac{d\mathbf{k}}{(2\pi)^3} \psi_j^*(\mathbf{k} + \mathbf{q}) \psi_j(\mathbf{k})$$

denotes the form factor. The sum over  $j$  of  $F_j(\mathbf{k}'_\pi - \mathbf{k}_\pi)$  yields  $Z$  times the charge form factor for the nucleus  $F(\mathbf{k}'_\pi - \mathbf{k}_\pi)$ , where  $F(0) = 1$ .

As is commonly done in the study of pion-nucleus scattering, we shall, at this point, introduce separable interactions to represent the elementary pion-nucleon scattering amplitude in the  $l=0$  and  $l=1$  channels, the

only relevant ones at the energies considered here. In the  $l=0$  case, the scattering matrix reads

$$\langle \mathbf{r}''_\pi - \mathbf{r} | t^s(E) | \mathbf{r}_\pi - \mathbf{r} \rangle = D_s(E) v_s(|\mathbf{r}''_\pi - \mathbf{r}|) v_s(|\mathbf{r}_\pi - \mathbf{r}|) \quad (3.6)$$

with

$$D_s(E) = \lambda_s \left[ 1 + \frac{\lambda_s}{\alpha_s} \frac{\bar{\mu}}{4\pi} (\alpha_s + iq_0)^2 \right]^{-1}$$

for a Yamaguchi form factor

$$v_s(r) = \frac{[\alpha_s^2 + q_0^2] e^{-\alpha_s r}}{4\pi r} \quad (3.7)$$

or, in momentum space,

$$v_s(q) = \frac{\alpha_s^2 + q_0^2}{\alpha_s^2 + q^2}, \quad (3.8)$$

where  $q_0 = \sqrt{2\bar{\mu}E}$  is the on-shell momentum. We introduce the convolution product  $\tilde{G}_s$  of the strong-interaction form factor with the free Green's function

$$\begin{aligned} \tilde{G}_s(\mathbf{r}') &= \int d\mathbf{r} v_s(r) G_0(|\mathbf{r}' - \mathbf{r}|) \\ &= \frac{2\bar{\mu}}{4\pi r} (e^{-\alpha_s r} - e^{iq_0 r}). \end{aligned} \quad (3.9)$$

Then we can reexpress Eq. (3.5a) in the form

$$\begin{aligned} \tilde{\Delta}_c^s(E, \mathbf{r}'_\pi, \mathbf{r}_\pi) &= D_s(E) \int d\mathbf{r} \rho(r) V_c(|\mathbf{r}'_\pi - \mathbf{r}|) \\ &\quad \times \tilde{G}_s(|\mathbf{r}'_\pi - \mathbf{r}|) v_s(|\mathbf{r}_\pi - \mathbf{r}|), \end{aligned} \quad (3.10)$$

where

$$\rho(r) = \frac{1}{Z} \sum_{j=1}^Z |\psi_j(r)|^2$$

denotes the single-particle state proton density normalized to 1.

To obtain the result for the pion-nucleon  $p$  wave it is easier to go through the momentum space representation

where the pion-nucleon transition matrix now reads

$$\langle \mathbf{k} | t^p(E) | \mathbf{k}' \rangle = D_p(E) \mathbf{k} \cdot \mathbf{k}' v_p(k) v_p(k') \quad (3.11)$$

with

$$v_p(q) = (\alpha_p^2 + q_0^2) / (\alpha_p^2 + q^2) \quad (3.12)$$

and

$$D_p(E) = \lambda_p \left[ 1 + \lambda_p \frac{\bar{\mu}}{6\pi} [\alpha_p (3q_0^2 + \alpha_p^2) + 2iq_0^3] \right]^{-1} \quad (3.13)$$

Replacing in (3.5b) the matrix element of  $t(E)$  by its expression (3.12), we have

$$\bar{\Delta}_c^p(E, \mathbf{k}'_\pi, \mathbf{k}_\pi) = Z D_p(E) F(\mathbf{k}'_\pi - \mathbf{k}_\pi) v_p(k_\pi) J(\mathbf{k}'_\pi, \mathbf{k}_\pi) \quad (3.14)$$

with

$$J(\mathbf{k}'_\pi, \mathbf{k}_\pi) = \int \frac{d\mathbf{k}}{(2\pi)^3} V_c(|\mathbf{k}'_\pi - \mathbf{k}|) \mathbf{k}_\pi \cdot \mathbf{k} \tilde{G}_p(k) \quad (3.15)$$

and

$$\tilde{G}_p(k) = v_p(k) G_0(k) \quad (3.16)$$

Equation (3.15) is then transformed to

$$J(\mathbf{k}'_\pi, \mathbf{k}_\pi) = i \int d\mathbf{r} h'(r) \mathbf{k}_\pi \cdot \hat{\mathbf{r}} e^{i\mathbf{k}'_\pi \cdot \mathbf{r}} \quad (3.17)$$

where  $\hat{\mathbf{r}}$  is a unit vector ( $\hat{\mathbf{r}} = \mathbf{r}/r$ ) and we have introduced

the auxiliary function,  $h(r)$ , defined by the relation

$$\frac{dh(r)}{dr} = V_c(r) \frac{d\tilde{G}_p(r)}{dr} \quad (3.18)$$

We thus obtain

$$J(\mathbf{k}'_\pi, \mathbf{k}_\pi) = \mathbf{k}_\pi \cdot \mathbf{k}'_\pi \int d\mathbf{r} h(r) e^{i\mathbf{k}'_\pi \cdot \mathbf{r}} \\ = \mathbf{k}_\pi \cdot \mathbf{k}'_\pi L_p(k'_\pi) \quad (3.19)$$

and the  $p$ -wave static-plus-closure result reads

$$\bar{\Delta}_c^p(E, \mathbf{k}'_\pi, \mathbf{k}_\pi) \\ = Z D_p(E) F(\mathbf{k}'_\pi - \mathbf{k}_\pi) \mathbf{k}_\pi \cdot \mathbf{k}'_\pi v_p(k_\pi) L_p(k'_\pi) \quad (3.20)$$

To obtain  $L_p(k'_\pi)$  we have to solve the first-order differential equation (3.18) which defines the function  $h(r)$  and compute the Fourier transform or, equivalently, starting from Eq. (3.19):

$$L_p(k'_\pi) = -\frac{4\pi}{k'_\pi} \int_0^\infty r^2 dr h'(r) j_1(k'_\pi r) \\ = \frac{4\pi}{k'_\pi{}^2} \int_0^\infty r^2 dr \Delta h(r) j_0(k'_\pi r) \quad (3.21)$$

with  $j_0(k'_\pi r)$ ,  $j_1(k'_\pi r)$  denoting the spherical Bessel functions of order zero and one, and  $\Delta h(r)$  denotes the Laplacian of the (scalar) function  $h(r)$ .

From (3.20) one can now obtain the coordinate-space representation of the  $p$ -wave result which reads

$$\bar{\Delta}_c^p(E, \mathbf{r}'_\pi, \mathbf{r}_\pi) = \frac{1}{2} D_p(E) \int d\mathbf{r} [v_p(r) \Delta \rho(\mathbf{r} + \mathbf{r}_\pi) h(|\mathbf{r} + \boldsymbol{\delta}|) - v_p(r) \rho(\mathbf{r} + \mathbf{r}_\pi) \Delta h(|\mathbf{r} + \boldsymbol{\delta}|) - \Delta v_p(r) \rho(\mathbf{r} + \mathbf{r}_\pi) h(|\mathbf{r} + \boldsymbol{\delta}|)] \quad (3.22)$$

with  $\boldsymbol{\delta} = \mathbf{r}_\pi - \mathbf{r}'_\pi$ . This expression is easily obtained by writing in (3.20)

$$\mathbf{k}_\pi \cdot \mathbf{k}'_\pi = \frac{1}{2} [k_\pi^2 + k'_\pi{}^2 - (\mathbf{k}_\pi - \mathbf{k}'_\pi)^2] \quad (3.22)$$

It should be clear that for large values of  $r'_\pi$ , the matrix elements (3.10) and (3.22) fall at least like  $1/r'_\pi{}^2$ , one factor coming from the Green's function and the other from the Coulomb potential. The results (3.10) and (3.22) will be used in the numerical calculations presented in Sec. IV where we will introduce a finite-range Coulomb potential.

We now have to subtract the ground-state contributions in order to obtain the correct Coulomb excitation potential. Hence in Eqs. (3.4) we reinterpret the intermediate-state summation,  $\alpha$  so that it runs only over those states occupied in the ground state. Because we are working within the framework of a single-particle approximation for the description of the nuclear target, with distinguishable particles, the only contribution arises from the term in which  $\alpha = j$ :

$$\bar{\Delta}_{c,0}(E, \mathbf{r}'_\pi, \mathbf{r}_\pi) = \sum_{j=1}^Z H_j(r'_\pi) \int d\mathbf{r}'_\pi d\mathbf{r}_N G_0(|\mathbf{r}'_\pi - \mathbf{r}'_\pi|) \psi_j^*(\mathbf{r}_N) \langle \mathbf{r}'_\pi - \mathbf{r}_N | t(E) | \mathbf{r}_\pi - \mathbf{r}_N \rangle \psi_j(\mathbf{r}_N) \quad (3.23a)$$

with

$$H_j(r'_\pi) = \langle \mathbf{r}'_\pi \psi_j | V_c | \mathbf{r}'_\pi \psi_j \rangle = \int d\mathbf{r} |\psi_j(r)|^2 V_c(|\mathbf{r}'_\pi + \mathbf{r}|) \quad (3.23b)$$

Let us remark that if we were considering identical particles, then transitions among the occupied orbitals within the ground state (i.e., those with  $\alpha \neq j$ ), forbidden by the Pauli exclusion principle, would also have to be removed. Then for large  $r'_\pi$ , the lowest-order Coulomb potential  $V_c(\mathbf{r}'_\pi, \mathbf{r}_N)$  becomes independent of  $\mathbf{r}_N$ , and the orthogonality of the nuclear single-particle orbitals requires  $\alpha = j$  so that those forbidden transitions would not contribute asymptotically. The leading power in  $1/|\mathbf{r}'_\pi|$  cancels between the contributions from Eqs. (3.5) and (3.23). This is most clearly seen in the coordinate-space representation where Eq. (3.4), with the approximations mentioned above, can be reexpressed as

$$\bar{\Delta}_c(E, \mathbf{r}'_\pi, \mathbf{r}_\pi) = \sum_{j=1}^Z \int d\mathbf{r}_N [V_c(\mathbf{r}'_\pi - \mathbf{r}_N) - H_j(r'_\pi)] \psi_j^*(\mathbf{r}_N) S(\mathbf{r}'_\pi - \mathbf{r}_N, \mathbf{r}_\pi - \mathbf{r}_N) \psi_j(\mathbf{r}_N) \quad (3.24a)$$

where we have introduced, to simplify the notation, the auxiliary quantity

$$S(\mathbf{r}'_{\pi}-\mathbf{r}_N, \mathbf{r}_{\pi}-\mathbf{r}_N) = \int d\mathbf{r}''_{\pi} G_0(\mathbf{r}'_{\pi}-\mathbf{r}''_{\pi}) \times \langle \mathbf{r}''_{\pi}-\mathbf{r}_N | t(E) | \mathbf{r}_{\pi}-\mathbf{r}_N \rangle . \tag{3.24b}$$

Note also that the monopole term which is the dominant piece at large  $r'_{\pi}$  in the expansion

$$1/|\mathbf{r}'_{\pi}-\mathbf{r}_N| = \sum_l \frac{1}{r'} \left[ \frac{r <}{r >} \right]^l P_l(x) \tag{3.25}$$

for a pointlike Coulomb potential or its equivalent in the finite-range Coulomb potential, cancels between the two pieces.

For the case of  $^{16}\text{O}$  we have calculated the results for the pion-nucleon  $s$  wave in a mixed  $(\mathbf{k}_{\pi}, \mathbf{r}_{\pi})$  representation to display this cancellation explicitly and show the relative importance of the monopole piece. For this case the target states are  $l=0$  and  $l=1$  and the “transitions” to be removed are 0-0, 1-1. The 0-0 case leads to only a monopole piece while the 1-1 leads to a monopole and quadrupole contribution. In Fig. 1 we show the results for closure only, the full subtraction and the case of the monopole subtraction only. Clearly, while this correction

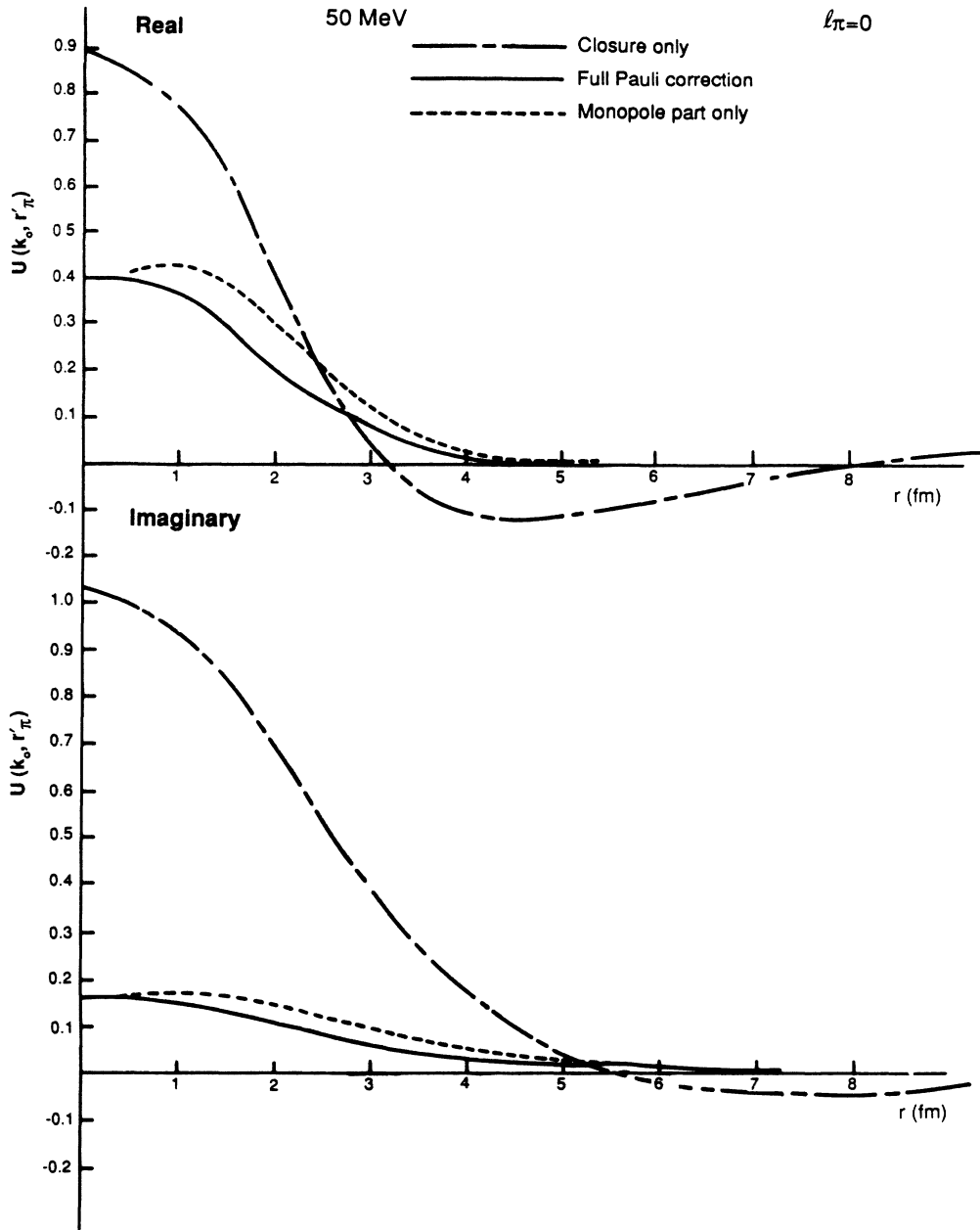


FIG. 1. The Coulomb excitation  $s$ -wave contribution in a mixed representation. The closure approximation results [Eq. (3.11), dashed-dotted curves] are compared with those including the monopole subtraction [Eq. (3.32), dashed curves] and those including the full subtraction [Eq. (3.34), solid curves].

is essential for large  $r$ , the retention of the monopole subtraction part alone is a reasonable approximation. In Appendix B we derive the explicit coordinate-space expressions for the Coulomb excitation correction including the monopole subtraction for both  $s$ - and  $p$ -wave interactions.

#### IV. RESULTS

We have performed numerical calculations at three energies (50, 110, and 180 MeV) for the  $^{40}\text{Ca}$  nucleus. To evaluate the strong optical potential (2.9) as well as the Coulomb excitation contribution one needs the single-particle wave functions. Unless otherwise specified, the density for  $^{40}\text{Ca}$  was constructed of single-particle orbitals  $1s$ ,  $1p$ ,  $2s$ , and  $1d$  obtained by the solution of the Schrödinger equation with a Woods-Saxon potential adjusted to reproduce the electron-scattering data (6) (with the inclusion of the finite size of the proton charge distribution). This density, referred to as the “standard” one, has an r.m.s. radius equal to 3.445 fm. The corresponding potential strengths and binding energies are shown in Table I. To have a measure of the size of effects to be expected from a variation in neutron vs proton radius, a second density was constructed by simply taking a larger radius for the potential well. This second density (the “big” density) has an r.m.s. radius of 3.555 fm and a slightly larger skin thickness. It has no direct physical significance and is used only to provide a scale for density changes. The two densities are shown in the upper right-hand corner of Fig. 2. The ordinary Coulomb potential was taken to be that given by the measured charge density (6).

The Coulomb excitation contribution is computed from the coordinate-space expressions (B6) and (B7), which include the monopole subtraction. These expressions have been symmetrized by including the two contributions which correspond to whether the excitation or deexcitation occurs via the Coulomb potential [see Eq. (3.1)]. The nonlocality is due to the presence of both the long-range Coulomb potential and the Green’s function propagator as may be checked easily, for example, in Eq. (B6) by introducing the zero-range limit on the strong form factor. In addition, (B6) and (B7) have a long-range dependence on the pion coordinate, in either of the two variables, which decreases as  $1/r^3$ . Although they do not depend on the modulus of the difference of the two vec-

TABLE I. Depths and binding energies used for the calculation of the standard  $^{40}\text{Ca}$  bound single-particle wave functions and density. The half-radius of the Woods-Saxon density is given by  $1.4 A^{1/3}$  fm and the diffusivity was taken to be 0.5 fm. The rms radius of the density is 3.445 fm. The depths of the wells were adjusted slightly to improve the agreement with the electron-scattering charge form factors.

1	$n$	$N$	$V(\text{MeV})$	$E_B(\text{MeV})$	$R_{rms}(\text{fm})$
0	1	4	40	31.6	2.80
0	2	4	40	12.2	3.74
1	1	12	50	32.7	3.24
2	1	20	40	14.7	3.82

tors  $r_\pi$  and  $r'_\pi$ , rotational symmetry implies that these contributions can be expressed as a function of  $r_\pi, r'_\pi$  and the cosine of the angle between them. The projection of the Coulomb excitation contributions onto partial waves is made as the function is constructed. The inner three-dimensional integral is performed numerically with Gauss-Laguerre and Gauss-Legendre methods. This technique is very slow and for future calculations it may be desirable to devise more efficient methods.

The scattering amplitudes are evaluated by using a fully nonlocal optical-model code with finite range pion-nucleon  $t$  matrices [see Eqs. (3.6) and (3.12)]. The value of the off-shell range parameter was fixed at 300 MeV/c for the pure strong potential and potential strengths were obtained using the methods of Ref. 23, including binding and Pauli blocking but in the static approximation.<sup>29</sup> True absorption is treated by the addition of a potential proportional to  $\rho^2$ .

Before introducing any explicit Coulomb contribution, we evaluate for reference the differential cross sections for the pure strong optical potential with the standard and big densities as defined above. The results are shown in Fig. 2 for 50, 110, and 180 MeV pion incident kinetic energies. The big density yields minima which appear at smaller angles: a typical order of magnitude is a shift of about 0.5–1.0 degree for the first minimum and larger for the second minimum in the resonance region. These results may be interpreted to yield an indication of the differences between the  $\pi^+$  and  $\pi^-$  cross sections if the  $\pi^+$  is assumed to scatter only from protons and the  $\pi^-$  from neutrons whenever the neutron and proton distribution have an r.m.s. radius difference of the order of 0.11 fm. Although the dominance of the 3-3 resonance provides support for such an assumption, the correction for the actual relative cross sections is energy dependent and would lead to a more realistic reference of the order of 0.15 fm.

The first and simplest contribution of the Coulomb interaction is the addition of the Coulomb potential to the strong optical potential. Hence the effective potential that enters the Schrödinger equation reads schematically

$$U(E) + V_c .$$

This is actually the standard prescription used in the literature<sup>30</sup> in most phenomenological analysis of the intermediate energy-scattering data. This simple contribution naturally leads to differences in the positions of minima between  $\pi^+$  and  $\pi^-$ . In Table I one observes that the positions of the minima are shifted towards larger angles for  $\pi^+$  and towards smaller angles for  $\pi^-$ . In fact, the effective potential felt by the  $\pi^-$  becomes more attractive while that felt by the  $\pi^+$  becomes more repulsive than in the absence of the Coulomb potential. This trivial, although essential, Coulomb contribution results in differences in the positions of the  $\pi^+$  and  $\pi^-$  minima which in general are smaller, especially for  $\pi^-$  than those resulting from the difference in the big and standard densities.

The second effect is the “Coulomb energy shift,” briefly discussed in Sec. II (Eq. (2.6b)), associated with

Coulomb rescatterings in the excited intermediate states [Eqs. (A9)]. Following usual approximate treatments of this correction,<sup>6,8</sup> we replace the operator shift by a constant energy shift and the effective potential to be includ-

ed in the Schrödinger equation is then

$$U(E - \langle V_c \rangle) + V_c .$$

To obtain an estimate, we have used a single number (7

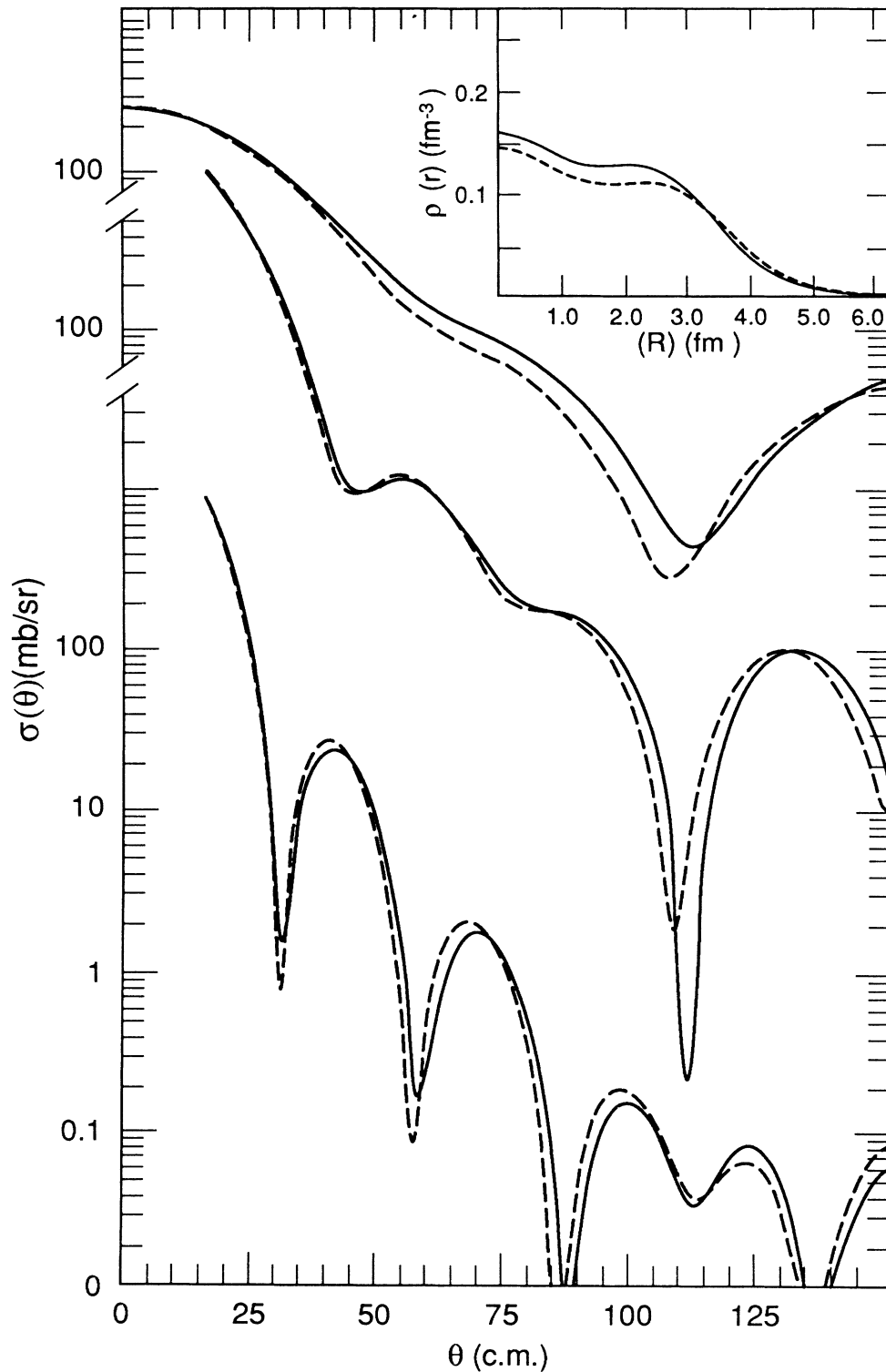


FIG. 2. Angular distributions for scattering for the two densities used for comparison. The two densities used for setting scales in the variation of the minimum positions of the angular distributions are shown in the upper right-hand corner. The solid curve shows the "standard" one and gives a body form factor in agreement with electron scattering. The dotted curve represents the "big" density used for comparison.



MeV, the approximate magnitude of the Coulomb potential at the surface of the  $^{40}\text{Ca}$  nucleus) for an effective energy shift. The effect of this simple Coulomb energy shift is shown in Table II and illustrated in Fig. 3 for  $\pi^+$ . The shift of the energy argument in the optical potential gives rise, by itself, to rather small changes on the angular distributions as can be inferred from Table II. There is a noticeable energy dependence of the effects associated to this contribution. Table II shows that, relative to the preceding calculation, the minima for  $\pi^-$  scattering are shifted to smaller angles below the resonance and to larger angles above and vice versa for  $\pi^+$  scattering. This reflects a partial energy-dependent compensation between the shift  $\langle V_c \rangle$  and the Coulomb potential  $V_c$ . It should also be remarked, looking at Fig. 3, that for  $\pi^+$  scattering below resonance the minima are filled while they are deepened at 180 MeV. The opposite effect is observed for  $\pi^-$  scattering. The global effect of the Coulomb energy shift in the elastic differential cross sections is similar for the two pion charges. A detailed analysis<sup>7,8</sup> based on this prescription for the optical potential has shown a definite improvement of the agreement with the data around the resonance region for the relative differences of the  $\pi^+$  and  $\pi^-$  elastic differential cross sections as well as for the corresponding isotopic differences for the  $^{16}\text{O}$  and  $^{18}\text{O}$  nuclei.

We show in Fig. 4 the differential ratios (the relative differences of the cross sections divided by the average) with and without the contribution of virtual Coulomb excitation, i.e., for a corresponding effective potential:

$$U(E - V_c) + V_c + \Delta_c .$$

They display in a conspicuous way the changes in the cross sections arising from this effect. At all energies they are very small for  $\pi^-$  both in magnitude and for the displacement of the minima. On the contrary, for  $\pi^+$

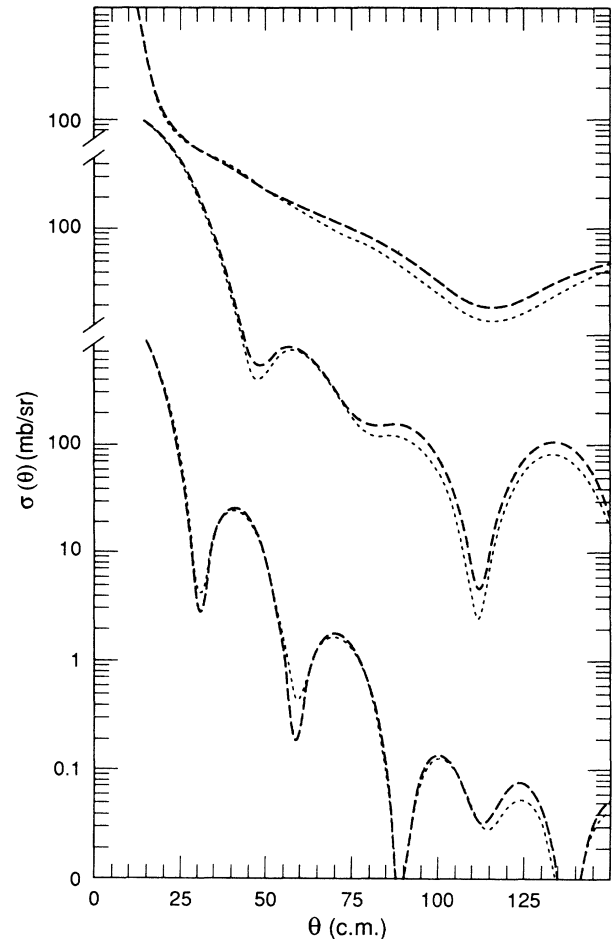


FIG. 3. The effect of the Coulomb energy shift alone, comparing calculations with (dashed) and without (dotted) the energy variations ( $\pm 7$  MeV for  $\pi^+$ ).

TABLE II. Minimum positions obtained for the angular distributions calculated with the pure strong and energy shifted optical potentials, with and without the Coulomb potential. In the first two columns, the notations "small" and "big" refer, respectively, to the standard density (Table I) and to the density with the larger r.m.s. radius of 3.55 fm. Also given are minimum positions obtained in the calculation of the angular distributions when the Coulomb excitation contribution is included.

	$U(E)$		$U(E) + V_c$	$U(E - V_c) + V_c$	$U(E - V_c) + V_c + CX$
	Standard	Big			
	$\pi^+$				
50 MeV	111.7(0.45)	107.5(0.30)	115.3(1.43)	114.8(1.94)	114.1(2.23)
110 MeV	46.5(9.44)	45.5(9.42)	47.3(3.92)	48.1(5.38)	48.2(4.30)
				82.0(1.51)	82.7(1.46)
180 MeV	110.8(0.02)	107.7(0.02)	111.3(0.03)	111.7(0.05)	111.9(0.06)
	31.1(0.91)	30.5(0.87)	31.7(4.65)	31.5(2.75)	31.7(3.52)
	58.4(0.13)	56.9(0.09)	59.3(0.62)	58.9(0.17)	59.2(0.22)
	87.7(0.000)	85.7(0.003)	88.8(0.005)	88.7(0.000)	89.3(0.000)
	$\pi^-$				
50 MeV	111.7(0.45)	107.5(0.30)	110.1(0.04)	112.1(0.003)	112.5(0.004)
110 MeV	46.5(9.44)	45.5(9.42)		45.7(14.53)	45.8(15.24)
	110.8(0.02)	107.7(0.02)	110.1(0.07)	109.4(0.08)	109.7(0.08)
180 MeV	31.1(0.91)	30.5(0.87)	30.8(0.09)	30.9(0.05)	30.9(0.03)
	58.4(0.13)	56.9(0.09)	57.6(0.004)	58.0(0.09)	57.9(0.08)
	87.7(0.000)	85.7(0.003)	86.8(0.009)	86.8(0.000)	86.7(0.000)

they are sizeable as can also be seen in Fig. 5 which show the differential cross sections. At 180 MeV the effect is primarily seen in the minima since the scattering is diffractive. All together the effect of the Coulomb excitation correction is smaller than that arising from the Coulomb energy shift as anticipated. It cannot be mocked up by a constant modification of the Coulomb energy shift itself.

Comparing the shifts due to the Coulomb excitation effect with those from the change in density and using the scale of 0.11 fm one can estimate that corrections to the radii extracted of the order of 0.02 to 0.03 fm might be expected.

At this point, one may ask how reliable the evaluation of the Coulomb excitation contribution is, how it could influence the analysis of nuclear sizes using pion scattering and if corresponding corrections can be made in the data analysis. For this latter to be true it must be possible to calculate the Coulomb excitation potential to an appropriate accuracy. To this end we have investigated some of the consequences due to uncertainties in the physical inputs to this quantity. We have studied the dependence of the Coulomb excitation correction on the

off-shell range of the pion nucleon and matrix and on the finite-size charge distribution of the nucleon and we conclude that they do not induce any significant uncertainties in the evaluation of the Coulomb excitation contribution.

Finally, we discuss the role of the monopole subtraction in our calculations. To do this we evaluate the Coulomb excitation contribution within the closure approximation [Eqs. (3.11) and (3.21)]. The closure approximation is expected to be more reliable at the higher energies. The monopole subtraction is essential in obtaining a correct evaluation of the Coulomb excitation contribution by forcing the long-range behavior of this correction

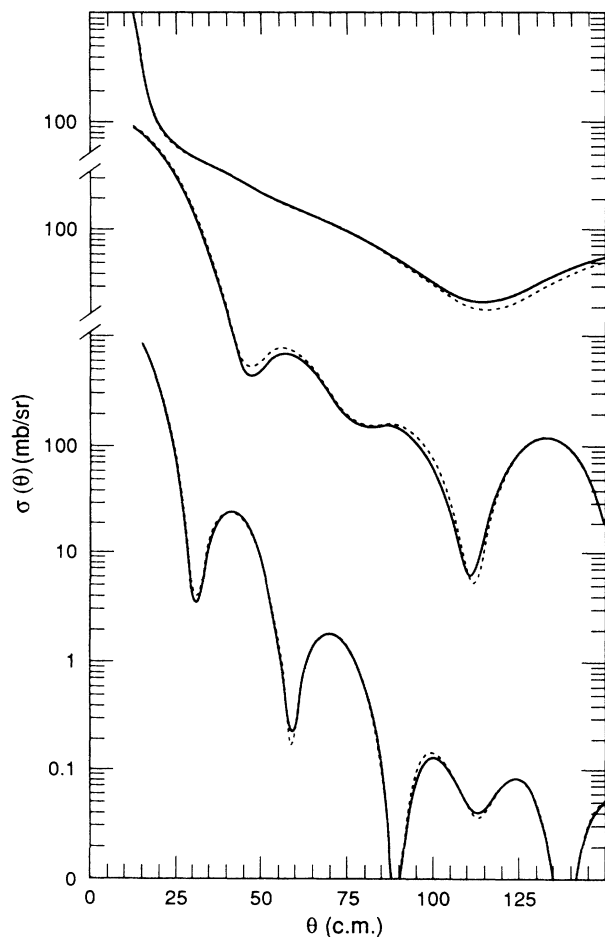


FIG. 4. Comparison of differential cross sections with both energy shift and Coulomb excitation (solid) with that including only the energy shift (dotted).

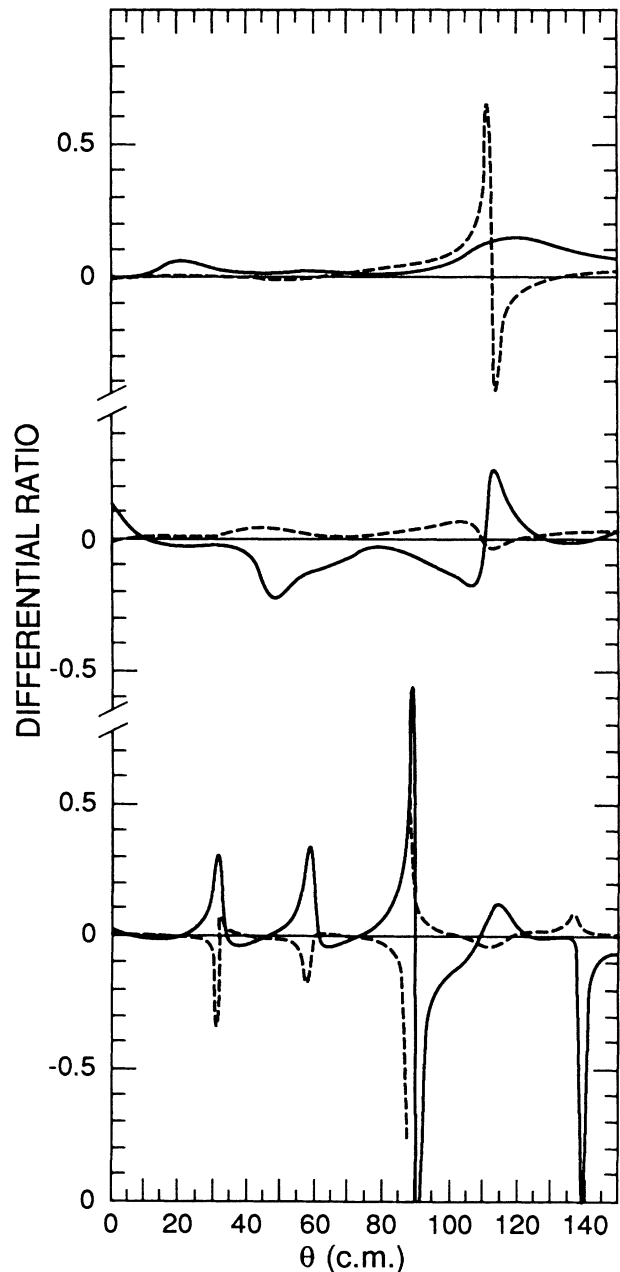


FIG. 5. Same comparison as in Fig. 4 but for the difference in the cross sections compared with their average.

to be  $1/r^3$  instead of  $1/r^2$ . At the lower energies, i.e., around 50 MeV, the monopole subtraction is presumably a rather crude estimate of the subtraction really required, especially since Pauli correlations should play an important role there. We are confident, on the other hand, that our estimates of the corrections to closure for the Coulomb excitation contributions around and above 100 MeV are adequate.

## V. SUMMARY AND CONCLUSIONS

The first part of this work has been devoted to a formal analysis of the role of the Coulomb interaction in optical potential approaches to multiple-scattering theories. One has first to include the Coulomb potential in the Schrödinger equation. Then the optical potential is modified in two ways: the coherent intermediate-state Coulomb rescattering leads to a shift of the energy argument at which the optical potential must be evaluated while the virtual Coulomb excitations give rise to a second branch of corrections. These contributions are usually neglected in multiple-scattering calculations at intermediate energies.

Since the Coulomb energy shift has already been discussed in the literature,<sup>1,9</sup> we have concentrated our efforts mainly on the virtual-Coulomb-excitation contribution. Within a first-order theory for the optical potential, we have derived in Sec. III practical expressions for these contributions to lowest order in the Coulomb interaction. To derive the expressions (B6) and (B7), which should be considered as corrections to the optical potential, we introduced a static approximation and neglected binding corrections as well as Pauli correlations. No direct comparison with data is attempted at this stage and we have only compared theoretical evaluations done within the same framework.

To illustrate our theoretical construction we have then used our expressions to calculate  $\pi^+$  and  $\pi^-$  scattering on  $^{40}\text{Ca}$ . To judge the magnitude of the effects due to the Coulomb excitation contributions, we have compared the resulting differential cross sections with those arising from standard calculations currently used in the literature<sup>30</sup> where the Coulomb potential is simply added to the strong optical potential as well as those obtained when including the energy shift. The size of the contribution of the virtual Coulomb excitations to the differential cross sections is not negligible compared to that arising from the Coulomb shift of the effective reaction energy. Clearly lower energies involve different dynamics, as is well known, e.g., at 50 MeV the main features of the angular distributions arise from the pion-nucleon  $s$ - and  $p$ -wave interference.<sup>31</sup> The  $\pi^+$  angular distributions show sizeable contributions at most energies. The comparison with the reference calculations which evaluates the differential cross sections for two densities with r.m.s. radii differing by 0.11 fm suggests a contribution to the radii extracted of  $\sim 0.02$ – $0.03$  fm.

To analyze the scattering data one should however start from a more realistic strong optical potential which should incorporate the effects of recoil. To obtain more precise bounds on the uncertainties in the neutron distri-

bution radii extracted from data, it is worthwhile to develop more efficient computational methods and theoretical improvements must be introduced. In particular, the treatment of the Coulomb energy shift, assumed here to be constant and equal to the surface value of the Coulomb potential, should be investigated more thoroughly. The momentum dependence neglected could partially affect the results of a neutron radius extraction. One should, at the same level, in the virtual-Coulomb-excitation contribution, improve on the monopole subtraction and try to include some nonstatic corrections. A step in that direction could be to treat the 3-3 channel without a static approximation as is done in the  $\Delta$ -hole model calculations.<sup>32</sup>

## ACKNOWLEDGMENTS

This work was supported in part by the U.S. Department of Energy. Financial support from our institutions allowed the regular meeting necessary for the completion of this work. This Division de Physique Theorique is a research unit of the Universities Paris 11 and 6 associated with the CNRS.

## APPENDIX A

We provide here the exact derivation of the optical potential in the presence of a Coulomb's projectile interaction. We want to calculate the elastic scattering amplitude  $T(E)$  from the target ground state. Using projection operators ( $P_0$  projecting onto the ground state while  $Q_0 = 1 - P_0$  projects onto the excited states of the target), we have

$$P_0 T(E) P_0 = P_0 (V_N + V_C) [1 + G_0(E) T(E)] P_0, \quad (\text{A1})$$

where the various operators entering here have been defined [in Eq. (2.2)]. The ground-state optical potential is defined by the integral equation

$$P_0 T(E) P_0 = P_0 [V_C + U(E)] P_0 [1 + G_0(E) P_0 T(E)] P_0. \quad (\text{A2})$$

Straightforward manipulations show that  $U(E)$  can be explicitly written in integral form

$$U(E) = V_N + (V_N + V_C) Q_0 G_0(E) Q_0 [U(E) + V_C]. \quad (\text{A3})$$

Similarly, the pure (i.e., in the absence of the Coulomb interaction of the projectile) strong optical potential fulfills the relation:

$$U_N(E) = V_N + V_N Q_0 G_0(E) Q_0 U_N(E). \quad (\text{A4a})$$

Equivalently we may write

$$U_N(E) = \Lambda_N V_N = V_N \tilde{\Lambda}_N, \quad (\text{A4b})$$

where we have introduced the strong distortion operators

$$\Lambda_N = 1 + U_N(E) G_0(E) Q_0 \quad \text{and} \quad \tilde{\Lambda}_N = 1 + Q_0 G_0(E) U_N(E). \quad (\text{A4c})$$

The strong Green's function  $G_N(E)$  is given by

$$G_N(E) = (E + i\delta - H_0 - Q_0 V_N Q_0)^{-1} \quad (\text{A5a})$$

$$= G_0(E) + G_0(E) Q_0 V_N Q_0 G_N(E) \quad (\text{A5b})$$

$$= G_0(E) + G_0(E) Q_0 U_N(E) Q_0 G_0(E) \quad (\text{A5c})$$

such that

$$Q_0 G_N(E) = Q_0 G_0(E) \Lambda_N = \tilde{\Lambda}_N G_0(E) Q_0 = G_N(E) Q_0. \quad (\text{A5d})$$

Starting now from Eq. (A3), multiplying on the left by  $\Lambda_N$ , solving then for  $Q_0 U(E)$  and projecting on the ground state we obtain the rigorous result,

$$\begin{aligned} P_0 U(E) P_0 = & P_0 U_N(E) P_0 + P_0 \Lambda_N Q_0 V_C Q_0 \frac{1}{1 - Q_0 G_N(E) Q_0 V_C Q_0} Q_0 \Lambda_0 \tilde{\Lambda}_N P_0 + P_0 \Lambda_N Q_0 \frac{1}{1 - Q_0 V_C Q_0 G_N(E) Q_0} V_C P_0 \\ & + P_0 V_C Q_0 \frac{1}{1 - Q_0 G_N(E) Q_0 V_C Q_0} Q_0 \tilde{\Lambda}_N P_0 + P_0 V_C Q_0 G(E) Q_0 V_C P_0. \end{aligned} \quad (\text{A6})$$

It is clear that this projection may be separated into three contributions:

$$P_0 U(E) P_0 P_0 U_N(E) P_0 + P_0 \Delta_N(E) P_0 + P_0 \Delta_C(E) P_0. \quad (\text{A7})$$

The leading term is the pure strong optical potential. The first correction term,  $P_0 \Delta_0(E) P_0$ , resumes all of the contributions that involve at least one transition from or to the ground state via the Coulomb interaction: i.e., the last three terms on the rhs of Eq. (A6); we then call these contributions Coulomb excitation corrections.

$$\begin{aligned} P_0 \Delta_C(E) P_0 = & P_0 U_N(E) Q_0 (E - H_0 - Q_0 V_C \tilde{\Lambda}_N Q_0)^{-1} Q_0 V_C P_0 + P_0 V_C Q_0 (E - H_0 - Q_0 \Lambda_N V_C Q_0)^{-1} Q_0 \Lambda_N V_C P_0 \\ & + P_0 V_C Q_0 (E - H_0 - Q_0 \Lambda_N V_C Q_0)^{-1} Q_0 U_N(E) P_0. \end{aligned} \quad (\text{A8})$$

The last correction term,  $P_0 \Delta_N(E) P_0$ , involves initial and final strong transitions from and to the target ground state with intermediate state Coulomb and strong optical distortions. It represents the modification of the strong optical potential due to intermediate-state Coulomb re-scattering and it is given directly by the second term on the rhs of Eq. (A6). It would be the only modification if there were no Coulomb transitions from and to the ground state. It is indeed an easy matter to realize that the first two terms of the right-hand side of Eq. (A8) recombine to yield a strong optical potential with a Coulomb shifted energy argument, i.e.,

$$\begin{aligned} P_0 U_N(E - Q_0 V_C Q_0) P_0 = & P_0 U_N(E) P_0 \\ & + P_0 U_N(E) Q_0 G_0(E) Q_0 V_C Q_0 \\ & \times \frac{1}{1 - Q_0 G_N(E) Q_0 V_C Q_0} \\ & \times Q_0 G_0(E) Q_0 U_N(E) P_0 \end{aligned} \quad (\text{A9})$$

and

$$P_0 \Delta_N(E) P_0 = P_0 U_N(E - Q_0 V_C Q_0) P_0 - P_0 U_N(E) P_0. \quad (\text{A10})$$

## APPENDIX B

To develop the full coordinate-space form it is no longer sufficient to use the density (or the ground-state form factor in the momentum space representation) as was done in the closure expression (3.10) and (3.22). We must introduce the explicit form of the wave functions

$$\psi_j(\mathbf{r}) = R_{nl}(r) Y_l^m(\hat{\mathbf{r}}), \quad (\text{B1})$$

where  $R_{nl}(r)$  is the radial part of the wave function. Following the discussion in Sec. III, we will consider the monopole subtraction,  $H_j^{(0)}(\mathbf{r}'_\pi)$ , i.e., we retain in  $H_j(r'_\pi)$  only its monopole contribution from Eq. (3.23). Denoting by  $V_c^0(r'_\pi, r_\pi)$  the monopole part of the Coulomb potential whose expansion reads

$$V_c(|\mathbf{r}'_\pi - \mathbf{r}_\pi|) = \sum_{L=0}^{\infty} V_c^L(r'_\pi, r_\pi) P_L(\hat{\mathbf{r}}'_\pi \cdot \hat{\mathbf{r}}_\pi) \quad (\text{B2})$$

it is straightforward to obtain ( $H_{nl}^{(0)} = H_j^{(0)}$ )

$$H_{nl}^{(0)}(\mathbf{r}'_\pi) = \frac{1}{4\pi} \int_0^\infty r^2 dr R_{nl}^2(r) V_c^0(r'_\pi, r) \quad (\text{B3})$$

or, equivalently,

$$H_{nl}^{(0)}(\mathbf{r}'_\pi) = \frac{1}{4\pi} \int d\mathbf{r} R_{nl}^2(r) V_c(|\mathbf{r}'_\pi - \mathbf{r}|). \quad (\text{B4})$$

Since we consider only closed-shell nuclei, we can easily perform the  $m$  summation in (3.22) and (B24) since  $m$  only appears in the product  $\psi_j(\mathbf{r}_N) \psi_j^*(\mathbf{r}_N)$ . We obtain

$$\bar{\Delta}_c(E, \mathbf{r}'_\pi, \mathbf{r}_\pi) = \sum_{nl} \frac{2l+1}{4\pi} \int d\mathbf{r} \left[ V_c(\mathbf{r}'_\pi - \mathbf{r}) - \frac{1}{4\pi} \int d\mathbf{r}' R_{nl}^2(r') V_c(|\mathbf{r}'_\pi - \mathbf{r}'|) \right] R_{nl}^2(r) S(\mathbf{r}'_\pi - \mathbf{r}, \mathbf{r}''_\pi - \mathbf{r}) . \quad (\text{B5})$$

The sum on  $(n, l)$  is over the occupied proton orbitals. The  $s$ -wave Coulomb excitation correction, within the static approximation, in coordinate space, can thus be expressed as

$$\bar{\Delta}_c^s(E, \mathbf{r}'_\pi, \mathbf{r}_\pi) = D_s(E) \sum_{nl} \frac{2l+1}{4\pi} \int d\mathbf{r} [V_c(|\mathbf{r}'_\pi - \mathbf{r}|) - H_{nl}^{(0)}(\mathbf{r}'_\pi)] R_{nl}^2(r) \bar{G}_s(|\mathbf{r}'_\pi - \mathbf{r}|) v_s(|\mathbf{r}_\pi - \mathbf{r}|) . \quad (\text{B6})$$

We proceed in a similar way to derive the corresponding  $p$ -wave Coulomb excitation correction and obtain [compare with Eq. (3.22)]:

$$\begin{aligned} \bar{\Delta}_c^p(E, \mathbf{r}'_\pi, \mathbf{r}_\pi) = \frac{1}{2} D_p(E) \sum_{nl} \left[ \frac{2l+1}{4\pi} \int d\mathbf{r} \{ v_p(r) \Delta R_{nl}^2(|\mathbf{r} + \mathbf{r}_\pi|) [h(|\mathbf{r} + \boldsymbol{\delta}|) - H_{nl}^{(0)}(\mathbf{r}'_\pi) \bar{G}_p(\mathbf{r} + \boldsymbol{\delta})] \right. \\ \left. - v_p(r) R_{nl}^2(|\mathbf{r} + \mathbf{r}_\pi|) [\Delta h(|\mathbf{r} + \boldsymbol{\delta}|) - H_{nl}^{(0)}(\mathbf{r}'_\pi) \Delta \bar{G}_p(|\mathbf{r} + \boldsymbol{\delta}|)] \right. \\ \left. - \Delta v_p(r) R_{nl}^2(|\mathbf{r} + \mathbf{r}_\pi|) [h(|\mathbf{r} + \boldsymbol{\delta}|) - H_{nl}^{(0)}(\mathbf{r}'_\pi) \bar{G}_p(|\mathbf{r} + \boldsymbol{\delta}|)] \right] , \quad (\text{B7}) \end{aligned}$$

i.e., we have simply replaced in (3.22)  $h(r)$  by  $[h(r) - H_{nl}^{(0)}(r) \bar{G}_p(r)]$  and  $\rho(r)$  by

$$\sum_{nl} \frac{2l+1}{4\pi} R_{nl}^2(r) .$$

These expressions (B6) and (B7) will be used in the numerical calculations developed in Sec. IV where we use a coordinate-space optical potential numerical code. Finally, if needed, it is not difficult to include the full, rather than the monopole, subtraction in Eq. (3.24). With the same notation, (B5) would be transformed to

$$\bar{\Delta}_c(E, \mathbf{r}'_\pi, \mathbf{r}_\pi) = \sum_{nl} \frac{2l+1}{4\pi} \int d\mathbf{r} \left[ V_c(\mathbf{r}'_\pi - \mathbf{r}) - (2l+1) \sum_L \begin{pmatrix} l & l & L \\ 0 & 0 & 0 \end{pmatrix}^2 P_L(\hat{\mathbf{r}} \cdot \hat{\mathbf{r}}'_\pi) H_{nl}^L(r'_\pi) \right] R_{nl}^2(r) S(\mathbf{r}'_\pi - \mathbf{r}, \mathbf{r}''_\pi - \mathbf{r}) , \quad (\text{B8})$$

where

$$\begin{pmatrix} l & l & L \\ 0 & 0 & 0 \end{pmatrix}$$

is a 3- $j$  coefficient, and

$$H_{nl}^L(r'_\pi) = \int_0^\infty r^2 dr R_{nl}^2(r) V_c^L(r'_\pi, r) . \quad (\text{B9})$$

$V_c^L$  denoting the  $L$ th order term of the multipole expansion of the Coulomb potential (B2). The full subtraction thus involves a slightly more complex structure than the monopole subtraction (B5). Yet, it does not represent any overwhelming difficulty since the  $L$  summation is constrained to very few terms, at least for  $^{16}\text{O}$  and  $^{40}\text{Ca}$ , by the 3- $j$  coefficient.

\*Mailing address: Laboratoire de Physique Nucléaire, T 14/24 5 étage, Université Paris 7, 2 place Jussieu, F-75251 Paris CEDEX 05, France.

<sup>1</sup>G. Fäldt and H. Pilkuhn, Phys. Lett. **40B**, 613 (1972); **46B**, 337 (1973).

<sup>2</sup>J. F. Germond and C. Wilkin, Phys. Lett. **688**, 229 (1977); Ann. Phys. (N.Y.) **121**, 285 (1979).

<sup>3</sup>R. Jäckle, H. Pilkuhn, and H. G. Schlaile, Phys. Lett. **76B**, 177 (1978).

<sup>4</sup>M. B. Johnson and H. A. Bethe, Comments Nucl. Part. Phys. **8**, 75 (1978).

<sup>5</sup>J. Fröhlich, H. Pilkuhn, and H. G. Schlaile, Phys. Lett. **121B**, 235 (1983).

<sup>6</sup>J. Hüfner, Nucl. Phys. **B58**, 55 (1973).

<sup>7</sup>J. P. Dedonder, Thèse d'Etat, Orsay, France, 1979 (unpublished).

<sup>8</sup>J. P. Dedonder, J. P. Maillet, and C. Schmit, Ann. Phys. (N.Y.) **127**, 1 (1980).

<sup>9</sup>T. E. O. Ericson and L. Tauscher, Phys. Lett. **112B**, 425 (1982).

<sup>10</sup>F. Cannata and J. P. Dedonder, Nuovo Cimento **76A**, 468 (1983).

<sup>11</sup>T. E. O. Ericson and J. Hüfner, Nucl. Phys. **B67**, 205 (1972); J. F. Dubach, E. J. Moniz, and G. D. Nixon, Phys. Rev. C **21**, 729 (1979).

<sup>12</sup>J. Fröhlich, B. Saghai, C. Fayard, and G. M. Lamot, Nucl. Phys. **A435**, 738 (1985). In the framework of the three-body problem, a large amount of work has been devoted to the treatment of the Coulomb interaction; see, for instance, the

- talks by E. O. Alt, J. L. Friar, V. F. Karchenko, and S. P. Merkuriev in *Proceedings of the International Conference on the Theory of Few-Body and Quark-Hadronic Systems*, Dubna, U.S.S.R., 1987, edited by V. K. Lukyanov (Joint Institute for Nuclear Research, Dubna, 1987).
- <sup>13</sup>M. J. Jakobson *et al.*, Phys. Rev. Lett. **38**, 1201 (1977); J. Jansen *et al.*, Phys. Lett. **77B**, 359 (1978).
- <sup>14</sup>R. R. Johnson *et al.*, Phys. Rev. Lett. **43**, 844 (1979).
- <sup>15</sup>J. P. Egger *et al.*, Phys. Rev. Lett. **39**, 1608 (1977); B. M. Freedom *et al.*, Phys. Rev. C **23**, 1136 (1981); S. H. Dam *et al.*, *ibid.* **25**, 2574 (1982); K. G. Boyer *et al.*, *ibid.* **29**, 182 (1984).
- <sup>16</sup>W. R. Gibbs and B. F. Gibson, Annu. Rev. Nucl. Part. Sci. **37**, 411 (1987).
- <sup>17</sup>D. Ashery *et al.*, Phys. Rev. C **23**, 2173 (1981).
- <sup>18</sup>K. Nakai *et al.*, Phys. Rev. Lett. **44**, 1446 (1980).
- <sup>19</sup>Note: It is difficult to treat the annihilation contribution in a fully consistent way in a standard multiple-scattering approach [however, see H. Garcilazo and W. R. Gibbs, Nucl. Phys. **A381**, 487 (1981)]. Here we treat it in a phenomenological way via additional density-dependent terms which certainly influence the values of extracted radii.
- <sup>20</sup>K. M. Watson, Rev. Mod. Phys. **30**, 565 (1958); A. K. Kerman, H. McManus and R. M. Thaler, Ann. Phys. (N.Y.) **8**, 551 (1959).
- <sup>21</sup>F. Cannata, J. P. Dedonder, and F. Lenz, Ann. Phys. (N.Y.) **143**, 84 (1982).
- <sup>22</sup>H. Garcilazo and W. R. Gibbs, Nucl. Phys. **A356**, 284 (1981).
- <sup>23</sup>W. B. Kaufmann and W. R. Gibbs, Phys. Rev. C **28**, 1286 (1983).
- <sup>24</sup>L. S. Kisslinger, Phys. Rev. **98**, 761 (1955).
- <sup>25</sup>W. R. Gibbs, in *Common Problems in Low- and Medium-Energy Nuclear Physics*, edited by B. Castel, B. Goulard, and F. C. Khanna (Plenum, New York, 1979), p. 595.
- <sup>26</sup>I. Sick *et al.*, Phys. Lett. **B88**, 245 (1979); J. B. Bellicard *et al.*, Phys. Rev. Lett. **19**, 527 (1967).
- <sup>27</sup>Jaap de Kam, thesis, University of Amsterdam, 1981; Jaap de Kam, Nucl. Phys. **A360**, (1981); Phys. Rev. C **24**, 1554 (1981); **28**, 2176 (1983).
- <sup>28</sup>R. Hagaoka and K. Ohta, Phys. Rev. C **33**, 1393 (1986).
- <sup>29</sup>The recoil effects have been studied in detail in the context of local field corrections; see M. B. Johnson and B. D. Keister, Nucl. Phys. **A305**, 461 (78) and M. K. Banerjee and S. J. Wallace, Phys. Rev. C **21**, 1996 (1980). In these papers the static approximation is shown to yield a very large magnitude of the effects which are considerably reduced once recoil is included. Although different, there are some similarities to the present calculation.
- <sup>30</sup>See, e.g., O. Meirav *et al.*, Phys. Lett. **B 199**, 9 (1987); J. A. Carr, H. McManus, and K. Stricker-Bauer, Phys. Rev. C **25**, 952 (1982); R. Seki, K. Masutani, and K. Yazaki, *ibid.* **27**, 2817 (1983); E. R. Siciliano, M. D. Cooper, M. B. Johnson, and M. J. Leitch, *ibid.* **34**, 267 (1986).
- <sup>31</sup>W. R. Gibbs, B. F. Gibson, A. T. Hess, and G. J. Stephenson, Jr., Phys. Rev. C **13**, 2433 (1976); W. R. Gibbs, in *Theoretical Methods in Medium Energy and Heavy-Ion Physics*, edited by K. W. McVoy and W. A. Friedman (Plenum, New York, 1978), p. 503.
- <sup>32</sup>M. Hirata, F. Lenz, and K. Yazaki, Ann. Phys. (N.Y.) **108**, 116 (1977); M. Hirata, J. H. Koch, F. Lenz, and E. J. Moniz, *ibid.* **120**, 205 (1979); F. Lenz and E. J. Moniz, in *Advances in Nuclear Physics*, edited by J. W. Negele and Erich Vogt (Plenum, New York).